Journal of Biomedical Optics

SPIEDigitalLibrary.org/jbo

Coregistered photoacoustic-ultrasound imaging applied to brachytherapy

Tyler Harrison
Roger J. Zemp

Coregistered photoacoustic-ultrasound imaging applied to brachytherapy

Tyler Harrison and Roger J. Zemp
University of Alberta, Department of Electrical and Computer Engineering, 9107 116 Street, Edmonton, Alberta T6G 2V4 Canada

Abstract. Brachytherapy is a form of radiation therapy commonly used in the treatment of prostate cancer wherein sustained radiation doses can be precisely targeted to the tumor area by the implantation of small radioactive seeds around the treatment area. Ultrasound is a popular imaging mode for seed implantation, but the seeds are difficult to distinguish from the tissue structure. In this work, we demonstrate the feasibility of photoacoustic imaging for identifying brachytherapy seeds in a tissue phantom, comparing the received intensity to endogenous contrast. We have found that photoacoustic imaging at 1064 nm can identify brachytherapy seeds uniquely at laser penetration depths of 5 cm in biological tissue at the ANSI limit for human exposure with a contrast-to-noise ratio of 26.5 dB. Our realtime combined photoacoustic-ultrasound imaging approach may be suitable for brachytherapy seed placement and post-placement verification, potentially allowing for realtime dosimetry assessment during implantation. [DOI: 10.1117/1.3606566]

Keywords: photoacoustics; ultrasonics; medical imaging; real-time imaging.

Paper 11106LRR received Mar. 7, 2011; revised manuscript received Jun. 9, 2011; accepted for publication Jun. 10, 2011; published online Aug. 1, 2011.

Prostate cancer is a growing concern worldwide. While prostatectomy is a very effective method of treatment, the side-effects can be severe. One alternative treatment is brachytherapy, which is a targeted form of radiation therapy. Unlike traditional radiation therapies where a broad tissue area is exposed to a radioactive source, brachytherapy uses multiple sources to strongly target the tumor area with less impact to the surrounding tissue. The sources for brachytherapy take the form of tiny metallic seeds containing a radioisotope which are implanted in the body according to a treatment plan devised to deliver precise doses to the treatment area. Post-implantation, seed positions within the body relative to other tissues are ascertained in order to evaluate the success of the procedure. In some cases, additional seeds may need to be implanted.[1]

Imaging plays a vital role in both seed implantation and post-implantation dosimetry measures. Ultrasound is often used to guide needles for implantation because it can image the prostate well,[1] but needle guidance can be difficult, as incident ultrasound waves may be reflected away from the transducer face, degrading image quality. This same difficulty is also present when imaging brachytherapy seeds. Han et al. attempted ultrasound-only dosimetry, and discovered that seeds could only be identified about 74% of the time, with some physicians identifying more seeds than had been implanted.[2] Mamou and Feleppa have attempted to enhance seed detectability with ultrasound, but still have a high false–positive rate.[3] Therefore, other technologies such as CT and MR imaging are used for post-placement verification, but require bulky setups and potentially ionizing radiation. While these imaging modes work well for post-placement verification, manual coregistration with ultrasound is required to allow clinicians to perform treatment adjustments by implantation of further seeds.[1] These modalities are thus ill-suited for realtime applications.

Photoacoustic imaging is a noninvasive imaging modality that provides optical contrast with ultrasonic resolution by measuring pressure waves resulting from localized heating of a sample due to an incident short pulse-duration light source. This modality can be used with multiple wavelengths to separate contrast agents, such as oxy- and deoxy-hemoglobin,[4] the principal absorbers deep in tissue through visible wavelengths. While Erpelding et al.,[5] and Su et al.[6] have done work that indicates that photoacoustic imaging may be appropriate for needle guidance at multiple-centimeter depths, the ability to image smaller metallic objects like brachytherapy seeds has not been fully investigated, though the application has been proposed.[6] Brachytherapy seeds should have a broad absorption spectrum, so either multiwavelength imaging or a sufficiently long wavelength should provide good detection of these seeds. This would be a boon for both implantation and post-placement verification, potentially opening the door to realtime dosimetry calculations. Recent conference proceedings from our group and another lab have demonstrated brachytherapy seed imaging in chicken breast[7] and *ex vivo* dog prostate,[8] respectively. In this work, we quantitatively assess the suitability of photoacoustic imaging as a complementary modality to ultrasound for the purpose of brachytherapy seed detection at multiple wavelengths.

We evaluated the ability of photoacoustic imaging to form images of titanium-shelled 4.5-mm long by 0.8-mm diameter brachytherapy seeds (IAI-125A nonradioactive seeds, IsoAid LLC, Port Richey, Florida) by imaging at multiple wavelengths and optical penetration depths. Figure 1 shows the experimental setup. To compare the contrast of brachytherapy seeds to endogenous contrast, a tube (Intramedic™, BD, Franklin Lanes, New Jersey) of inner diameter 0.86 mm and length 4 cm was filled with rabbit blood, placed to the right of the seed, and both were enclosed in chicken breast tissue. Seeds were moved to different positions to simulate various optical penetration depths. This sample was placed in a plastic sample bath containing ~0.5 cm of water to maintain moisture in the tissue sample. Resulting realtime (5 frames/s) interleaved photoacoustic and flash ultrasound data were captured using a research ultrasound system (VDAS-I, Verasonics, Redmond, Washington) capable of 60 MHz capture on 64 parallel channels streamed to a host PC via PCI-Express.

Address all correspondence to: Roger Zemp, University of Alberta, Electrical and Computer Engineering, 9107 116 Street, Edmonton, Alberta T6G 2V4 Canada. Tel: 7804921825; E-mail: zemp@ece.ualberta.ca.

1083-3668/2011/16(8)/080502/3/$25.00 © 2011 SPIE

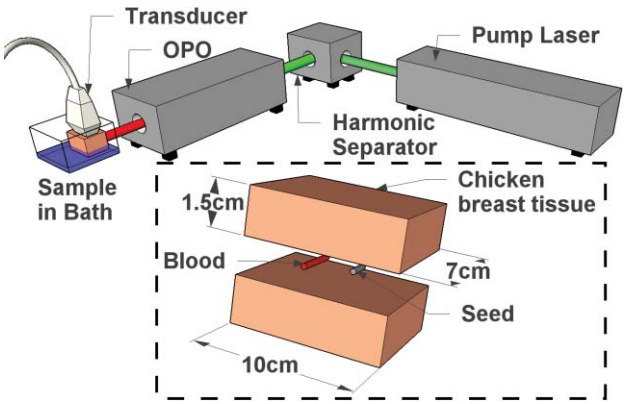

Fig. 1 System setup. Surelite III pump laser pumps Surelite OPO Plus optical parametric oscillator (Continuum, Santa Clara, California) providing tunable light at 650 to 900 nm. Incident light interrogates the sample which is in a water bath beneath the 128-element L7-4 38 mm (5 MHz center frequency, ~70% fractional bandwidth) linear array transducer (AT5L40B, Broadsound Corporation, Jupei City, Hsinchu, Taiwan). Inset: blown up sample setup with relevant dimensions.

Images were then reconstructed using delay-and-sum beamformers on the host PC. Photoacoustic images were thresholded at 40% of maximum intensity, and overlaid in a separate color scale. By viewing combined images and varying this threshold to eliminate endogenous signals, clinicians may be able to identify brachytherapy seeds *in vivo*. Multiwavelength imaging can give clinicians valuable information about not only seed location, but also vasculature around the tumor region. Figures 2(a) and 2(b) show how the seed can be seen with varying intensity levels compared to the blood sample at 760 and 797 nm. In these images, seed-to-blood contrast-to-noise (CNR) were 15 and −0.5 dB, respectively. The blood-filled tube appears as two surfaces in these images, whereas the seed appears as a continuous body. In the case of the blood-filled tube, signals are seen from the top and bottom surfaces: an effect in-part due to bandpass filtering effects of the ultrasound transducer. While this same effect should occur for the seed, the acoustic impedance mismatch of metal and tissue causes signals from the bottom

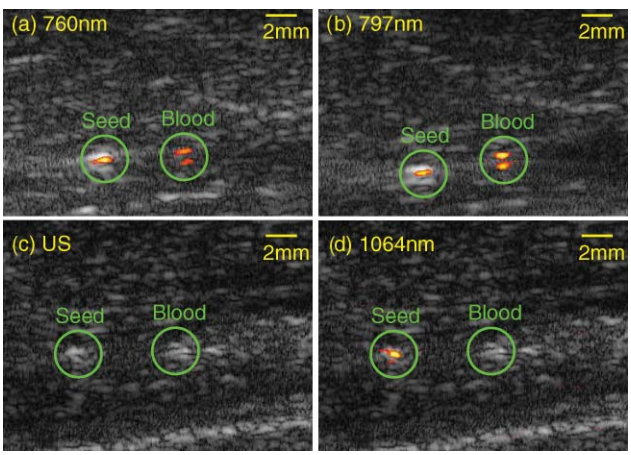

Fig. 2 (a) and (b) Combined ultrasound-photoacoustic images at a laser fluence of 20 mJ/cm^2 and a laser penetration depth of 2 cm. (c) and (d) Ultrasound and combined ultrasound-photoacoustic images at a fluence of 100 mJ/cm^2 and a laser penetration depth of 5 cm.

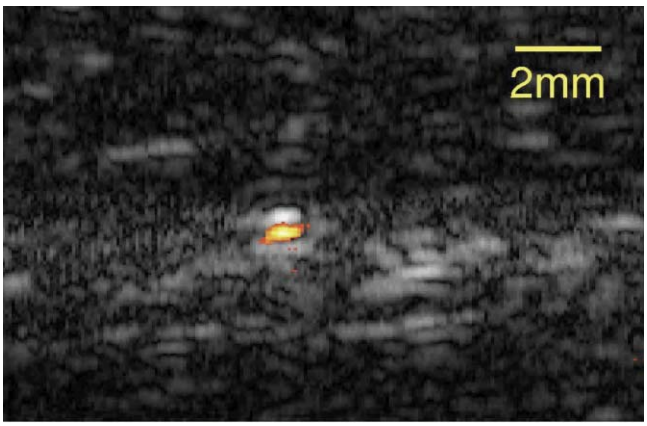

Video 1 Combined ultrasound-photoacoustic video at a laser fluence of 100 mJ/cm^2 and laser penetration depth of 5cm (MPEG, 1.1MB). [URL: http://dx.doi.org/10.1117/1.3606566.1]

surface propagating through the seed to be largely reflected by its top surface, reducing the signal received by the transducer.

Using the 1064 nm fundamental output of the pump laser, the blood-filled tube was indistinguishable from noise, while the brachytherapy seed provided a strong signal. Figures 2(c), 2(d), and Video 1 illustrate this: while the brachytherapy seed is indistinguishable from the blood-filled tube in the ultrasound image, the overlaid photoacoustic signal correctly identifies the seed. We found that the brachytherapy seeds were detectable using the ANSI exposure limit for fluence of 100 mJ/cm^2 at 1064 nm to a laser penetration of at least 5 cm with a CNR of 26.5 dB. Images are captured at a laser-repetition-rate-limited 5 frames/s and displayed in realtime, shown in Video 1 [Fig. 2(d)].

As further proof of the effectiveness of photoacoustic imaging for brachytherapy seed imaging, we generated receiver operating characteristic (ROC) curves of representative images for a few of the more promising wavelengths, shown in Fig. 3. ROC curves are formed by varying the threshold at which a seed is said to be detected, and measuring the true-positive and false-positive rates determined by fractions of pixels above the threshold within and without the seed region. The seed region is located by picking the maximum amplitude in an image and defining a true-scale seed mask around this region. The same mask is applied for both ultrasound and photoacoustic images. We verified that maximum signals were due to the seed by removal and re-imaging. Performance was characterized by the area under the curve (AUC), annotated in the legend.

Figure 2 illustrates that brachytherapy seeds are visible at an intensity similar to endogenous optical contrast. This indicates that separating them using absorption-spectrum-based processing techniques should be possible. Even more promising is higher-fluence imaging at 1064 nm, as in Fig. 2(d) and Video 1, which we have demonstrated at a depth suitable for this application using a safe laser fluence with an excellent CNR. This means that a single wavelength could potentially be used to uniquely identify brachytherapy seeds. The realtime nature of our imaging technique will prove important in clinical settings and may enable continuous feedback for seed position planning. Finally, Fig. 3 indicates that photoacoustic imaging at 1064 nm can offer improved classification performance compared to ultrasound alone.

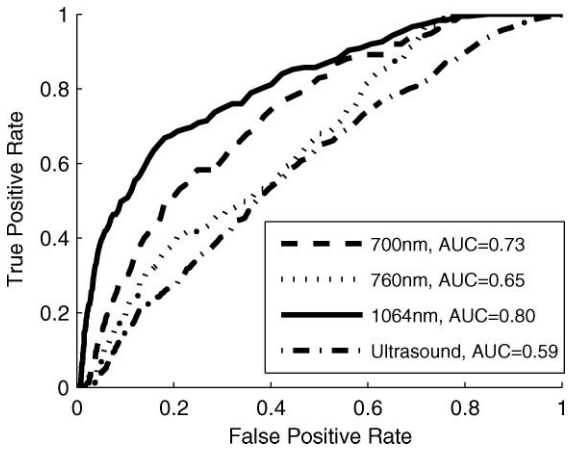

Fig. 3 Receiver operating characteristic curves for photoacoustic imaging at several wavelengths compared to ultrasound with AUC annotated in legend.

Chicken breast may not be an ideal tissue analogue for prostate tissue. Values for $\mu_a = 0.078$ mm^{-1} and $\mu_s' = 0.63$ mm^{-1} are typical for human prostate at 1064 nm.[9] While we were unable to find literature detailing the optical properties of chicken tissue at 1064 nm, values of $\mu_a \approx 0.2$ mm^{-1} and $\mu_s' \approx 0.05$ mm^{-1} have been reported for 1000 nm.[10] Applying $\mu_{\text{eff}} = (3\mu_a + \mu_s')^{1/2}$ to each substance, we get $\mu_{\text{eff}} = 0.41$ mm^{-1} for human prostate at 1064 nm and $\mu_{\text{eff}} = 0.39$ mm^{-1} for chicken tissue at 1000 nm. Using Beer's law, and assuming that μ_{eff} is roughly the same at 1064 and 1000 nm for chicken tissue, we get an expected reduction in signal intensity of 8.7 dB for a 5 cm depth image in prostate tissue compared to chicken breast. This would result in signal-to-noise ratio of 17.8 dB based on our prior measurement of 26.5 dB: more than adequate for imaging. While differences in absorption will impact the maximum imaging depth and anisotropy may impact detectability, our preliminary data motivates *in vivo* studies.

While the application of photoacoustic imaging to brachytherapy seems quite promising based on the data presented here, there are still several hurdles to overcome before this technology can be used in a clinical setting. Heating of the seed region is poorly understood, though it is likely to be highly localized and fast to dissipate. Local laser fluence may be unknown due to optical heterogeneity, impairing image quantification and quality. Light delivery to the prostate is further complicated by its location, likely requiring a rectal delivery probe. In clinical situations, light fluence and ultrasound attenuation should be accounted for in image reconstruction. A more rigorous study of multiwavelength imaging should be undertaken, as well as *in vivo* clinical studies.

Acknowledgments

We wish to acknowledge Dr. Keith Wachowicz for providing brachytherapy seeds. We gratefully acknowledge funding from NSERC (355544-2008, 375340-2009, STPGP 396444), Terry-Fox Foundation and the Canadian Cancer Society (TFF 019237, TFF 019240, CCS 2011-700718), the Alberta Cancer Research Institute (ACB 23728), the Canada Foundation for Innovation, Leaders Opportunity Fund (18472), Alberta Advanced Education and Technology, Small Equipment Grants Program (URSI09007SEG), Microsystems Technology Research Initiative (MSTRI RES0003166), University of Alberta Startup Funds, and Alberta Ingenuity/Alberta Innovates student scholarships.

References

1. D. B. Fuller, H. Jin, J. A. Kozial, and A. C. Feng, "CT-ultrasound fusion prostate brachytherapy: A dynamic dosimetry feedback and improvement method. A report of 54 consecutive cases," *Brachytherapy* **4**(3), 207–216 (2005).
2. B. Han, K. Wallner, G. Merrick, W. Butler, S. Sutlief, and J. Sylvester, "Prostate brachytherapy seed identification on post-implant TRUS images," *Med. Phys.* **30**(5), 898–901 (2003).
3. J. Mamou and E. J. Feleppa, "Ultrasonic detection and imaging of brachytherapy seeds based on singular spectrum analysis," *Acoust. Imaging* **29**(2), 127–132 (2009).
4. H. F. Zhang, K. Maslov, G. Stoica, and L. V. Wang, "Functional photoacoustic microscopy for high-resolution and noninvasive in vivo imaging," *Nat. Biotechnology* **24**(7), 848–851 (2006).
5. T. N. Erpelding, C. Kim, M. Pramanik, L. Jankovic, K. Maslov, Z. Guo, J. A. Margenthaler, M. D. Pashley, and L. V. Wang, "Sentinel lymph nodes in the rat: noninvasive photoacoustic and US imaging with a clinical US system," *Radiology* **256**(1), 102–110 (2010).
6. J. Su, A. Karpiouk, B. Wang, and S. Emelianov, "Photoacoustic imaging of clinical metal needles in tissue," *J. Biomed. Optics* **15**(2), 021309 (2010).
7. T. Harrison and R. J. Zemp, "Photoacoustic imaging of brachytherapy seeds using a channel-domain ultrasound array system," *Proc. SPIE* **7899**, 78990H (2011).
8. N. Kuo, H. J. Kang, T. DeJournett, J. Spicer, and E. Boctor, "Photoacoustic imaging of prostate brachytherapy seeds in *ex vivo* prostate," *Proc. SPIE* **7964**, 796409 (2011).
9. W. H. Nau, R. J. Roselli, and D. F. Milam, "Measurement of thermal effects on the optical properties of prostate tissue at wavelengths of 1,064 and 633 nm," *Lasers Surg. Med.* **24**(1), 38–47 (1999).
10. K. Ishii, N. Honda, T. Terada, and K. Awazu, "Determination of optical property changes during laser therapies," *Lasers and Electro Optics and The Pacific Rim Conference on Lasers and Electro-Optics, CLEO/PACIFIC RIM '09*, pp. 1–2 (2009).